Published in final edited form as:

FEBS Lett. 2015 November 14; 589(22): 3419–3432. doi:10.1016/j.febslet.2015.08.015.

Overcoming differences: the catalytic mechanism of metallo-β-lactamases

María-Rocío Meini[1], **Leticia I. Llarrull**[1,2,*], and **Alejandro J. Vila**[1,2,*]

[1]Área Biofisíca, Facultad de Ciencias Bioquímicas y Farmaceutícas, Universidad Nacional de Rosario, Suipacha 570, 200 Rosario, Argentina

[2]Instituto de Biología Molecular y Celular de Rosario (IBR, CONICET-UNR), Predio CONICET Rosario, 2000 Rosario, Argentina

Abstract

Metallo-β-lactamases are the latest resistance mechanism of pathogenic and opportunistic bacteria against carbapenems, considered as last resort drugs. The worldwide spread of genes coding for these enzymes, together with the lack of a clinically useful inhibitor, have raised a sign of alarm. Inhibitor design has been mostly impeded by the structural diversity of these enzymes. Here we provide a critical review of mechanistic studies of the three known subclasses of metallo- β-lactamases, analyzed at the light of structural and mutagenesis investigations. We propose that these enzymes present a modular structure in their active sites that can be dissected into two halves: one providing the attacking nucleophile, and the second one stabilizing a negatively charged reaction intermediate. These are common mechanistic elements in all metallo-β-lactamases. Nucleophile activation does not necessarily requires a Zn(II) ion, but a Zn(II) center is essential for stabilization of the anionic intermediate. Design of a common inhibitor could be therefore approached based in these convergent mechanistic features despite the structural differences.

Keywords

Metallo-β-lactamases; Mechanism; Antibiotic Resistance; Zinc enzymes; Drug Design

1 Introduction

β-Lactam antibiotics remain the most useful chemotherapeutic agents in the fight against bacterial infections. These antibiotics work by inhibiting penicillin-binding proteins (PBPs) implicated in bacterial cell wall biosynthesis, eventually causing cell lysis [1]. The clinical success of the first β-lactam in the 1950s, penicillin G (benzylpenicillin) led to the evolution

*Authors to whom correspondence should be addressed: llarrull@ibr-conicet.gov.ar; vila@ibrconicet.gov.ar; Tel.: +54-341-423 7070 (ext 637; 632); Fax: 54-341-4237070 (ext 607).
All the authors contributed equally to this work.

of different resistance mechanisms [2,3]. Increasing reports of resistance events prompted the search and development of related compounds with better and broader bactericidal action, giving rise to four types of β-lactam antibiotics in clinical use today: penicillins, cephalosporins, monobactams and carbapenems [4–6]. Despite much progress in antibiotic design, resistance to β-lactams is now a serious clinical problem, particularly in postsurgery, nosocomial infections and immunosuppressed patients [7,8].

The rapid advance of resistance has dampened the interest of pharmaceutical companies in investing in infectious diseases, leading to a substantial drop in the number of new antibiotics approved in the last years [9]. At present, there are very few new β-lactams in the pipeline and no new classes of antibiotics directed towards new targets available or in the pipeline [10]. Therefore, it is mandatory in the short term to find tools extending the useful life of available antibiotics [11].

1.1 Resistance mediated by β-lactamase enzymes

The most prevalent mechanism of resistance towards β-lactams is the expression of enzymes able to hydrolyze these antibiotics, namely β-lactamases. These enzymes catalyze the hydrolysis of the β-lactam ring characteristic of these antibiotics, rendering them inactive [1]. Most β-lactamases are known as serine-β-lactamases (SBLs) since they possess an essential Ser residue in their active site. These enzymes are evolutionarily related to penicillin binding proteins (PBPs) and have been grouped into three classes (A, C, and D) based on amino acid sequence alignments [1]. Metallo-β-lactamases (MBLs, or class B) are metalloenzymes with Zn(II) ions bound to the active site that are essential for their activity [12,13]. MBLs have an unusually broad substrate spectrum, being capable of hydrolyzing all classes of bicyclic β-lactam antibiotics (penicillins, cephalosporins and carbapenems). Though MBLs are not capable of recognizing and inactivating monobactams (monocyclic β-lactams), they are usually co-expressed with SBLs that hydrolyze these antibiotics. As a consequence, monobactams are not a plausible choice for the treatment of infections associated with MBLs production [12].

The inhibitors (clavulanic acid, tazobactam, and sulbactam) that are currently used in clinical settings in combination therapies with β-lactam antibiotics are mechanism-based inhibitors of SBLs [14]. The mechanistic differences with SBLs render MBLs resilient to inhibition by these compounds. The rational design of mechanism-based inhibitors against MBLs has been thwarted by the difficulty of finding common mechanistic features among different MBLs and for the different substrates, as we will discuss over this review [13].

In this sense, an understanding of the mechanism of MBLs, and in particular the entrapment and characterization of reaction intermediates, can give new hints on the structure of compounds that might bind to the active site and inhibit these enzymes. Such compounds might be used in combination with the existing β-lactam antibiotics prolonging their use to treat resistant bacteria.

1.2 Emergence of antibiotic resistance by metallo-β-lactamases

MBLs emerged in the last two decades as the major mechanism of resistance against carbapenems, last resort β-lactam antibiotics for the treatment of infections caused by

multiresistant pathogens [12]. Surprisingly, the first MBL (BcII from *Bacillus cereus*) was discovered by Sabath and Abraham in 1966, two decades before the clinical implementation of carbapenems. These authors showed that the cephalosporinase activity displayed by this strain could be inhibited by treatment with EDTA [15]. This wide-spectrum enzyme was initially considered a biochemical curiosity since it was found in a soil bacteria, being the only example of its kind along two decades. Notwithstanding, BcII became one of the workhorses for structural and mechanistic studies on MBLs [16–24]. This scenario changed in the 1980s when an increasingly large number of clinical isolates of *Bacteroides fragilis* [25], *Stenotrophomonas maltophilia* [26], various *Aeromonas* [27,28] and *Chryseobacterium* [29–31] species were found to express diverse chromosomally encoded Zn(II) β-lactamases. Among Gram negative bacteria, a silent gene coding for an MBL was found in *Bacillus anthracis* [32]. The situation became more worrisome when genes coding for MBLs were found in mobile genetic elements (which also harbor other resistance cassettes) in several Gram negative pathogens including members of the *Enterobacteriaceae* species, *Pseudomonas aeruginosa*, *Serratia marcescens* and the *Acinetobacter* species [8,12]. The association of MBL genes to these mobile genetic elements has facilitated the dissemination of these enzymes among prevalent pathogens, thus becoming a serious clinical threat. Outbreaks of pathogens producing the MBLs VIM-2 (Verona Integron-encoded Metallo-β-lactamase) and NDM-1 (New Delhi Metallo-β-lactamase) are rising in incidence all over the world, with high rates of death due to the lack of therapeutic options [33,34].

MBLs from environmental bacteria, initially considered as a mere curiosity, are now considered gene reservoirs which may be later transferred to opportunistic and pathogenic strains [35–37]. Recent studies revealed the presence of a wide variety of NDM-1-producing pathogens in public drinking water taps and seepages from New Delhi [38], revealing that the transmission of this gene has surpassed hospital barriers.

1.3 MBLs superfamily and classification

MBLs constitute a family of proteins belonging to an ancestral superfamily of metallohydrolases, all of them sharing a common αβ/βα sandwich scaffold and a metal-binding motif (His/Asn$_{116}$-X-His$_{118}$-X-Asp$_{120}$-His/Arg$_{121}$, His$_{196}$, Cys/Ser$_{221}$, His$_{263}$, according to the standard BBL numbering scheme [39]) located in the interface of the two αβ domains [40]. Members of this superfamily display a wide variety of activities, including human glyoxalase II, phosphodiesterase from *Escherichia coli*, parathion hydrolase from *Pseudomonas sp.*, N-acyl homoserine lactone hydrolase de *Bacillus thurigensis* and a human DNA nuclease; and a group of cytosolic redox proteins, among others [40]. Most of the non β-lactamase hydrolases present dinuclear sites containing Zn(II), Fe(II)/Fe(III) or Mn(II) ions, with an Asp/Glu$_{221}$ residue as a bridging ligand between the two metals. On the other side, MBLs lack a bridging protein residue; instead a water/hydroxide molecule occupies the bridging position while at position 221 a Cys or Ser residue is present [40].

The family of MBLs is divergent, with sequence identities as low as 10% or less in some cases. Even though, a classification in subclasses was performed based on sequence alignment guided by common structural features [39]. Subclass B1 and B3 MBLs are di-Zn(II) enzymes with a broad substrate profile (penicillins, cephalosporins and carbapenems)

[41–45]. The smaller subgroup B2, albeit phylogenetically closer to B1 enzymes [46], includes mono-Zn(II) enzymes capable of hydrolyzing exclusively carbapenems [47]. Subclass B1 enzymes exhibit sequence identities higher than 23% between their members [40]. This group includes almost all the clinically relevant MBLs: the aforementioned NDM [48] and VIM variants [49], in addition to IMP (Imipenemase) variants [50] SPM-1 (São Paulo Metallo-β-Lactamase) [51], acquired by pathogens through mobile genetic elements, apart from other endogenous MBLs like chromosome-borne *B. cereus* BcII [52], *B. fragilis* CcrA [53] or *Elizabethkingia meningoseptica* BlaB (β-lactamase B) [29]. The exclusive carbapenemases from subclass B2 share 11% sequence identity with B1 enzymes [40]. This group includes endogenous MBLs like *A. hydrophilia* CphA (Carbapenem-hydrolyzing metallo-β-lactamase) [54], *A. veronii* ImiS (Imipenemase from *A. veronii* bv. sobria) [28] and *Serratia fonticola* Sfh-I [36]. Finally, subclass B3 MBLs, the most distant in phylogenetic terms [46], comprises endogenous enzymes sharing only 9 residues with the rest of MBLs. Members of this group include chromosome-borne MBLs *Stenotrophomonas maltophilia* L1 [26], *E. meningoseptica* GOB [30] and *Legionella (Fluoribacter) gormannii* FEZ-1 [55]. The recently reported AIM-1 (Australian Imipenemase) represents the first B3 enzyme encoded in a mobile genetic element, suggesting that gene dissemination may not be limited to subclass B1 [56].

1.4 Active site structure of metallo-β-lactamases

The crystal structures of B1 and B3 enzymes have revealed dinuclear metal centers in the active site, comprised of two Zn(II) ions: one in a tetrahedral coordination sphere (Zn1 or M1 site) and one in a trigonal bipyramidal coordination sphere (Zn2 or M2 site) [18,42,43,57–59]. In B1 enzymes, the Zn(II) ion at the M1 site is coordinated to residues His116, His118 and His196 and a bridging water/hydroxide molecule (Wat1); while the Zn(II) ion at the M2 site is coordinated to residues Asp120, Cys221 and His263, the bridging water and an apical water molecule (Wat2). In B3 enzymes, the arrangement of the Zn2 site is modified with respect to B1 enzymes. These enzymes present a Ser residue at position 221 that does not participate in metal coordination. Instead, a His residue at position 121 completes the coordination sphere of the Zn2 site. Mutational analyses on B1 enzymes have shown that all metal binding residues are essential to provide full activity [19]. According to substrate binding experiments performed with BcII, the apo-enzyme is not able to bind β-lactam substrates, indicating that substrate binding in B1 MBLs is largely driven by electrostatic interactions with the metal ions [20]. Particularly, the interaction of the invariant β-lactam carboxylate moiety (at C3 in penicillins and carbapenems and C4 in cephalosporins) with Zn2 has been demonstrated by the crystallographic structures of enzyme-product (EP) complexes of MBLs representative of the three subclasses, as we will discuss later [59–61]. This carboxylate moiety also interacts with a highly conserved charged residue at position 224 in B1 and B2 enzymes and residues Ser221 and Ser223 in B3 enzymes [59–61].

B2 enzymes are fully active with a single Zn(II) ion localized in the M2 site, sharing the same ligand residues as in B1 enzymes, i.e., Asp120, Cys221 and His263 [47,62]. A naturally-occurring His116Asn substitution at the M1 site precludes Zn(II) from binding with high affinity, whilst in the presence of excess Zn(II), binding to this site can be

inhibitory [47]. A mutational analysis of the B2 enzyme CphA, showed that metal ligands Asp120, Cys221 and His263 are essential for the enzyme activity, as well as residues His118 and 196 [63].

The presence of residue Cys221 in B1 and B2 MBLs contrasts with the ubiquity of a Asp/Glu221 bridging ligand in other members of the MBL superfamily devoid of lactamase activity. The Cys ligand (despite being absent in B3 enzymes) is a hallmark of the active site of MBLs, since Cys residues are rarely found as Zn(II) ligands in exposed catalytic sites [64]. This is most striking considering that MBLs bind the Zn(II) cofactor in the oxidizing periplasmic space. The observation that B3 enzymes, lacking a Cys ligand, are phylogenetically closer to other members of the MBL superfamily [40] suggests that this residue confers an evolutionary advantage. Indeed, we recently demonstrated that a Cys residue in the metallic centers of B1 MBLs is critical for ensuring metal uptake in the periplasmic space of Gram-negative bacteria, leading to the active dinuclear enzyme [24].

2 Is it possible to establish a common catalytic mechanism for all MBLs?

β-Lactam hydrolysis involves a nucleophilic attack to the carbonyl group, the C-N bond cleavage and the protonation of the nitrogen. The bicyclic shape of β-lactams requires that both the nucleophilic attack and nitrogen protonation take place on the less hindered α side of the antibiotic molecule. So far, the central issues discussed on the mechanism of MBL-mediated catalysis have been: (1) whether these events occur in a concerted manner or in discrete steps with accumulation of reaction intermediates, (2) the identities of the nucleophile and the proton donor, and (3) the role of each Zn(II) ion in catalysis. Initial mechanistic schemes were proposed based on the well-known mechanism for β-lactam hydrolysis by Serine-β-lactamases (Figure 1A). In these enzymes, the attacking nucleophile is an activated Ser residue, that gives rise to a high energy transition state with a tetrahedral carbon (known as “tetrahedral intermediate”), in which the anionic charge developed is stabilized by a positively charged cleft in the active site, known as the “oxyanion hole”, by analogy to the one present in serine proteases. Cleavage of the C-N bond of the β-lactam occurs synchronously with protonation of the β-lactam nitrogen, resulting in formation of a covalent acyl-enzyme intermediate (Figure 1A). Attack by a catalytic water leads to another high-energy transition state. Finally, the rate-limiting deacylation step involves cleavage of the covalent bond between the β-lactam carbonyl and the oxygen of Ser70, coupled to the protonation step [14].

Mechanistic studies can make use of the classical methods: steady state kinetics, pre-steady state kinetics, site-directed mutagenesis and X-ray crystallography. In addition, the active site of Zn(II) enzymes can be selectively interrogated by X-ray Absorption Spectroscopy (XAS) and its variants, XANES and EXAFS. The requirement of synchrotron sources makes this technique less amenable to follow reactions in real time but, instead it has been extensively employed to trap reaction intermediates after Rapid Freeze-Quench (RFQ) of the reaction. Substitution of Zn(II) by divalent metal ions that are useful spectroscopic probes (mostly Co(II)) and preserve enzyme catalytic activity, has been extensively employed. These metal surrogates enable the use of additional techniques such as absorption

spectroscopy, EPR and NMR, either in real time or coupled with Rapid Freeze-Quench devices.

Clinically useful β-lactam antibiotics do not possess intrinsic chomophores, but several groups have exploited the use of synthetic chromophoric cephalosporins, such as nitrocefin, CENTA and chromacef. These compounds undergo intense spectroscopic changes upon hydrolysis that make them useful mechanistic probes. In this case, native Zn(II)-MBLs can be employed, but the spectral changes only give information on changes at the substrate molecule. Instead, Co(II) substitution allows monitoring changes on the enzyme active site during turnover, since characteristic bands corresponding to each metal-site can be followed in the UV-vis region.

Computational studies are challenging since transition metal ions are difficult to parametrize. The advent of density functional theory (DFT) provided the bases to perform reliable quantum mechanics (QM) and quantum mechanics-molecular mechanics (QM-MM) hybrid calculations on metalloenzymes [65]. Throughout this chapter we will describe how these approaches have contributed to the interpretation of experimental evidence.

2.1 Mechanism of B1 and B3 Metallo-β-lactamases

The dinuclear MBLs CcrA, IMP-1, BcII and NDM-1 (subclass B1) and L1 (subclass B3) are those whose catalytic mechanisms have been better characterized to date. We will focus our discussion on the pre-steady state mechanistic studies, together with structural evidence from the crystallographic structures of L1 and NDM-1 bound to hydrolyzed substrates. In addition, we will mention mutational analyses to assess the role on catalysis of amino acid residues located in the active site or in nearby loops.

2.1.1 Identities of the nucleophile and the proton donor—The two candidates proposed as the possible attacking nucleophile were the carboxylate group of the conserved residue Asp120 and the Zn(II)-bound hydroxide ion. Asp120 was early discarded as the nucleophile [17,66]. At present, the general consensus accepts that the Zn(II)-bound hydroxide ion is the attacking nucleophile, as it is the case for most Zn(II) hydrolases, in which the metal ion lowers the pKa of the bound water molecule [67–71]. The Zn1–Wat1 distance in B1 enzymes is typically 1.9–2.0 Å long, characteristic of a Zn(II)-bound hydroxide [72]; while the Zn2-Wat1 distance varies between 2.5 and 3 Å (Table 1) [18]. These data suggest that only Zn1 would be responsible of lowering the pKa. However, the finding that metal dissociation from the Zn2 site gave rise to an inactive enzyme led Page and coworkers to propose that the second Zn(II) ion was essential for activity [73,74]. These authors suggested that Zn2 contributes to lowering the pKa of the attacking nucleophile. However, a hydroxide moiety bridging two transition metal ions is expected to have less nucleophilic potency than a terminal hydroxide. A crystal structure of a BcII mutant showing that the short Zn1-Wat bond is preserved both in its mono- and dinuclear form [24] confirmed that the Zn2 ion is not required to provide an active nucleophile at neutral pH, at the same time supporting the idea of an attacking terminal hydroxide.

The identity of the proton donor is still not clear. Asp120 was originally proposed as the proton donor, being essential for activity in all MBL enzymes [75–79]. However, this

hypothesis requires transient dissociation of the carboxylate group from the metal ion upon protonation [80], a fact that has not been substantiated. The role of Asp120 as a proton donor was ruled out by a series of mutants on this position on BcII which showed a normal solvent kinetic isotope effect, therefore indicating that the rate-limiting step is a proton transfer in all cases [78]. The fact that k_{cat} is not significantly affected in the D120N mutant, indicates that Asp120 is not the proton donor in the rate-determining step [78]. These results were in agreement with those obtained with mutants on Asp120 position in the B3 MBL L1 [76]. Structural studies on Asp120 mutants suggest that, instead, its role is to adequately position Zn2 for substrate binding and catalysis [78,79,81]. Bounaga and Page have shown that BcII is inactivated at low pH by protonation of two residues, tentatively a Zn(II)-bound water molecule and Asp120 [17]. It was later shown that this inactivation at acidic pH is due to Zn(II) dissociation [82,83], as a consequence of protonation of Asp120. Based on this evidence, it seems unlikely that Asp120 might detach from the metal ion to be involved in a proton relay. An alternative proton donor candidate could be the carboxylic acid moiety formed upon β-lactam cleavage [59]. Instead, the most accepted hypothesis is that of a water molecule being the proton donor. These proposals will be analyzed in detail later.

2.1.2 Mechanistic studies on penicillin G hydrolysis using Co(II)-substituted enzymes—The substitution of the native Zn(II) ion by Co(II) in B1 MBLs gives rise to a characteristic UV-vis spectrum with a pattern of ligand field bands in the region between 500–650 nm, which present contributions of the metal ions in both sites, and a ligand-to-metal charge-transfer band (LMCT) around 340 nm corresponding to Cys→Co(II) bond from the Zn2 site [84–86]. The coordination number and geometry of the metal sites can thus be determined based on the electronic spectrum of the Co(II)-substituted enzymes both in the resting state and during turnover. In addition, Co(II)-substituted MBLs are slightly less active than the native Zn(II) variants, making them more amenable for trapping catalytic intermediates.

Mechanistic studies employing rapid-scanning stopped-flow techniques allow monitoring the spectral changes during turnover which are indicative of changes of the coordination sphere of the Co(II) ion during the reaction. Bicknell and Waley performed pioneering mechanistic studies on Co(II)-substituted BcII [16,87]. The authors documented the presence of two different enzyme-substrate (ES) complexes upon hydrolysis of penicillin G by following the reaction by means of electronic and MCD spectroscopy. A branched kinetic mechanism accounted for the observed kinetic data and ES complexes. These experiments were performed before the active site structure of these enzymes was known, and the results were interpreted by assuming a single Co(II) at the active site. Despite this fact, this work provided the first evidences of changes in the coordination geometry of the metal ions in the active site during turnover.

Steady state studies on the hydrolysis of penicillin G by Co(II)-BcII show a biphasic behavior, with an initial burst followed by a steady state rate [73]. Page and co-workers assigned the first burst to penicillin hydrolysis by di-Co(II) BcII, while the decrease observed in the reaction rate was attributed to the dissociation of one of the Co(II) ions during turnover, giving rise to a less active or inactive mono-Co(II) form. These experiments

were carried out following the spectral changes on the substrate, without monitoring the structural features of the enzyme active site.

We later reported a pre-steady state kinetics study aimed at addressing the activity of the different metal-loaded species of BcII [22]. Hydrolysis of penicillin G catalyzed by BcII samples with different Co(II)/BcII ratios was followed using a stopped-flow system associated to a photodiode array detector (PDA), considering the relative populations of the different species [84]. The kinetic data were better described by a branched kinetic pathway with two active species: di-Co(II) BcII and mono-Co(II) BcII. This model can also explain the biphasic progress curves previously observed by Page and coworkers [73], without assuming an inactive mono-Co(II) enzyme, as a result of re-equilibration of mono and di-Co(II) species after dilution on the reaction mix.

In the resting state, mono-Co(II) BcII is a mixture of a mono-Co(II) form at the M1 site and mono-Co(II) species at the M2 site in equilibrium [84]. The kinetic data on BcII is consistent with a mono-Co(II) active species with the metal ion localized in M2 site, although experimental studies on hydrolysis of cephalosporins by mono-Zn1 Bla2 [88], mono-Zn1 L1 [89] and calculations on mono-Zn1 BcII [90] support the existence of an active mono-Zn1 form. In the mono-Co(II)-M2 enzyme, the attacking nucleophile would be a water molecule activated by interactions with His118 and/or Asp120, similar to the mechanism proposed for mononuclear B2 enzymes [61,62], as we will discuss later.

No reaction intermediates could be trapped in penicillin hydrolysis by BcII, and the branched mechanism reported by Bicknell and Waley [16] could be assigned to the dinuclear enzyme. Structures were proposed for the two ES complexes based on the spectroscopic data [22]. The interactions proposed for ES^1 complex are in agreement with those observed in the enzyme-product (EP) complexes of penicillins and NDM-1 enzyme [44,59], while the interactions proposed for ES^2 account for the increase in coordination number of Co(II) as indicated by the spectroscopic data [22]. (Figure 1B) [22].

2.1.3 Mechanistic studies with cephalosporins—In 1998, Benkovic and coworkers reported that nitrocefin hydrolysis by the di-Zn(II) B1 enzyme CcrA proceeded with accumulation of a reaction intermediate with a strong absorption feature at 665 nm [66,91]. This band was attributed to an anionic enzymebound intermediate with a negatively charged nitrogen atom upon scission of the β-lactam C-N bond (EI, Figure 2A). The spectrum of this intermediate was reproduced by treating hydrolyzed nitrocefin with a strong base, strongly supporting this proposal [66]. Nitrocefin and chromacef hydrolysis by the di-Zn(II) B1 enzyme NDM-1 also take place with the accumulation of a similar intermediate [92]. This intermediate was also reported in nitrocefin hydrolysis by the B3 enzyme L1 [93]. RFQ-EPR of Co(II)-substituted L1 demonstrated that nitrocefin binding results in a change in the geometry of the Co(II) ions, providing evidence that the reaction intermediate is a metal-bound species [94]. RFQ-XAS on di-Zn(II) L1 also evidenced a significant lengthening of the Zn-Zn distance in this intermediate (from 3.42 in the resting state to 3.72 Å) [95]. QM/MM calculations [96] and model studies [97] supported the anionic structure of this intermediate, which features Zn2 bound to the negatively charged β-lactam nitrogen. This mechanism provided the first direct evidence of a catalytic role for the M2 site.

The rate-limiting step in this reaction is the decay of this intermediate, characterized by a solvent kinetic isotope effect of 2.9, consistent with the assignment of this decay to the protonation of the ring-opened nitrogen anion [91,98] (Figure 2A, EI →EP). This brings us back to the issue of the identity of the proton donor. As mentioned in Section 2.1.1, the most accepted hypothesis postulates a water molecule as the proton donor. One possibility is that an incoming water molecule from the bulk solvent is acidified by coordination to either one or both Zn(II) ions, hence providing the proton required to protonate the β-lactam nitrogen, regenerating the bridging nucleophile hydroxide [89]. However, it is not likely that water molecules can reach the active site once a substrate molecule is bound. Alternatively (Figure 2A), we propose that the proton donor is a water molecule bound to Zn2 in the resting state enzyme (W2) that shifts toward Zn1, replacing the vacant position left by the nucleophilic OH^-. This water molecule, bridging Zn1 and Zn2 in EI, is expected to have a low pKa, thus facilitating nitrogen protonation in an event which regenerates the nucleophilic hydroxide in EP. As shown in Figures 1 and 2, Asp120 can orient the bridging water to donate a proton to the intermediate. RFQ-EPR studies on the hydrolysis of chromacef by metal substituted NDM- 1 with Co(II) in the M1 site (CoCd-NDM-1) also showed that the M1 site undergoes a marked change in electronic structure upon reaction with substrate, indicative of a decrease in coordination symmetry and a rigid coordination sphere [86]. These results were interpreted as a five-coordinate Co(II) in the M1 site in EI, which could be attributed to simultaneous coordination of both O atoms from the newly formed carboxylate of the ring-opened intermediate (one from the μ-OH ligand, one from the substrate carbonyl; as proposed for ES^2 in Figure 1B for penicillin-hydrolysis), or by coordination of a water molecule. These observations suggest a role for the metal ion in the M1 site in nucleophile activation and/or delivery of the proton donor [86].

The π-conjugated electron-withdrawing substituent in nitrocefin stabilizes this anionic intermediate. Instead, the pKa of the ring nitrogen in hydrolysis products of penicillins and clinically relevant cephalosporins is expected to be much higher, suggesting that analogous intermediates are not to be expected for these substrates. However, DFT calculations on the mechanism of cefotaxime hydrolysis by di-Zn(II) CcrA [99] suggest that a Zn(II) ion in the M2 site would favor stabilization of a negative N5 atom upon nucleophilic attack and scission of the C-N bond. Steady state kinetic studies in di-Zn(II) BcII showed that the kinetic solvent isotope effect for k_{cat} was 1.4–1.6 for penicillin, cefuroxime, cephaloridine, and cefotaxime, suggesting that the rate-limiting step also involves proton transfer for these substrates [17,84]. These smaller values can be interpreted as reflecting the contribution of a metal-bound hydroxide (with an expected solvent effect of 0.7–0.8) together with proton transfer (with a solvent effect of 2.5–3.0) [100]. However, since these values correspond to steady state parameters, it is not possible to discard the existence of an anionic intermediate for these substrates only based on these data.

The role of the M2 site in this mechanism was confirmed by studying mono-Zn(II) variants. A mono-Co(II) L1 variant with the metal ion localized at the M2 site resulted inactive, while the mono-Zn(II) at M2 site analog could not be obtained [89]. On the other hand, mono-Zn(II) GOB is an active enzyme with the metal ion localized at the M2 site and displays a marked accumulation of this intermediate [101]. Spectroscopic data from hydrolysis of

chromacef by heterodimetallic forms of NDM-1 provided evidence of the binding of a moiety capable of absorbing delocalized spin density from the metal ion at the M2 site and a major role for Zn2 in electrophilic activation of the substrate and stabilization of the anionic intermediate [86].

Studies aimed at determining the role of the metal in the M1 site rely on pre-steady state studies under single-turnover conditions, since the existence of the mono- Zn(II) enzyme under steady-state conditions cannot be assured due to the metal concentration in Chelex-treated buffers. Unlike mono-Zn(II) enzymes with the metal localized at the M2 site, the mono-Zn1 forms of B1 and B3 enzymes do not stabilize the anionic intermediate. Pre-steady state studies with a mono-Zn(II) form of L1, with the metal ion localized at the M1 site, presented low activity against nitrocefin (5 % of the activity of di-Zn(II) L1), and did not stabilize the hydrolysis intermediate [89]. The B1 MBL Bla2 from *Bacillus anthracis* was purified with one Zn equivalent, localized at the Zn1 site according to EXAFS studies [88]. This protein preparation presented the peculiarity of being unstable when trying to saturate with Zn(II), precluding a comparative stopped-flow study on the di-Zn(II) enzyme. Mono-Zn1 Bla2 did not show accumulation of the nitrocefin intermediate, though it presented a considerable activity. Spectroscopic data on Bla2 indicates that Co(II) binds to the two sites with no preference, as is the case for BcII. An enzyme analog with 1 or 2 equivalents of Co(II) added accumulated the anionic intermediate. Based on the amount of the intermediate observed, the authors propose an equilibrium shift towards the di-Co(II) enzyme in the presence of substrate.

Hybrid Car-Parrinello QM/MM calculations were used to investigate the reaction mechanism of hydrolysis of cefotaxime by mono-Zn1 BcII [90]. The Zn1-bound water/hydroxyl is the attacking nucleophile and the calculations show that a second water molecule binds the zinc ion in the first step of the reaction, expanding the zinc coordination number and providing a proton donor adequately oriented for the second step. Asp120, Cys221, and His263 (which are ligands of Zn2 in the dinuclear enzyme) participate in a conserved hydrogen bond network in the active site, which initially contributes to orient the nucleophile, and then guides the second catalytic water molecule to the zinc ion after the substrate is bound. Cleavage of the β-lactam C-N bond occurs concomitantly with protonation of N5. The activation energy for the mechanism catalyzed by the mono-Zn(II) variant [90] was much higher than calculated for the di-Zn(II) enzyme [99], in agreement with the experiments showing that the active species in vivo is the dinuclear one [24].

This intermediate, however, can be elusive in some dinuclear enzymes: no accumulation or little was reported for BcII [102] or VIM-2 [85], while there are contradicting results for nitrocefin hydrolysis by IMP-1 by the Frère [103] and Crowder groups [104]. A second sphere mutation introducing a hydrogen bond with a metal ligand in BcII leads to stabilization of this intermediate, which is not observed in the native enzyme [105], disclosing that subtle changes between different MBLs also contribute to the stability of this EI species.

The accumulation of this intermediate is also affected by the dynamic of loops flanking the active site. Loop dynamics in MBLs has been probed by NMR [106–109], fluorescence of

engineered Trp residues [110], or double electron resonance (DEER) spectroscopy in spin-labeled samples [111,112]. Loop L3 is a short, mobile loop present in B1 enzymes (residues 56–66) that closes over the active site upon substrate binding, affecting catalysis [106–109]. Insertion of the B3 loop from IMP-1 into BcII resulted in accumulation of the intermediate [103]. A natural mutation in loop L10 (residues 220–237) in the allelic variant IMP-25 also leads to a more populated intermediate than in IMP-1. In the case of B3 enzymes, a study of mutations in loop L8 (residues 151–166) showed that loop motions correlated with the rate of formation of the nitrocefin intermediate [110]. Overall, these results demonstrate that, in addition to the presence of the Zn(II) ion at the M2 site, several additional factors contribute to the relative stabilization of this anionic intermediate.

2.1.4 Mechanistic studies with carbapenems—The mechanism of carbapenem hydrolysis, despite being the paradigmatic substrate of MBLs, has been less studied. Pre-steady state studies on imipenem hydrolysis by di-Zn(II) BcII revealed formation of a reaction intermediate absorbing at 380 nm. Co(II)- substitution allowed a more detailed characterization of this process. Di-Co(II) BcII hydrolyzes imipenem by a branched mechanism with accumulation of two reaction intermediates, one of them with a strong absorption at 407 nm [23]. RFQ-Resonance Raman experiments allowed assigning this band to a deprotonated form of a ring-opened pyrrolidine derivative (EI^1 in Figure 2B), which resembles the anionic intermediate identified in nitrocefin hydrolysis. The difference in the position of the absorption maxima when the reaction is performed with Co(II) or Zn(II)–BcII confirms the direct involvement of the metal ion in this intermediate.

Carbapenem hydrolysis is usually followed by tautomerization of the pyrrolidine double bond from Δ^1 to Δ^2 [113,114]. Both Zn(II)-BcII and Co(II)-BcII give rise to a Δ^1 product with a 7:3 diasteromeric ratio, which suggests a stereoselective protonation of the carbanionic species at C3 [23]. The proposed branched reaction mechanism includes two intermediates, EI^1 and EI^2 (Figure 2B). The nucleophilic attack gives rise to an open-ring derivative with a negative charge delocalized over a conjugated π system involving atoms N1 and C3. This anionic species (EI^1) is stabilized by direct interaction with Zn2. EI^1 can: (a) be protonated at N1 giving tautomer Δ^2, that once released to the aqueous milieu tautomerizes rapidly to its Δ^1 form giving a mixture of the α and β diasteromers; or (b) remain inside the enzyme pocket, favoring localization of the negative charge on C3 (EI^2). In the latter case, EI^2 could be protonated stereospecifically by a metal-bound water giving rise to an enzyme-product adduct (EI^3 or EP). This model accounts for the partial stereoselectivity.

DFT calculations showed that a stable intermediate species can be stabilized at the active site, with a delocalized negative charge encompassing the N1 and C3 atoms of the pyrrolidine ring and the Sulphur atom of the R2 substituent [23]. Recent QM-MM calculations on the reaction coordinate of hydrolysis of meropenem by NDM-1 by Nair and coworkers support formation of a stable anionic intermediate species [115].

A similar intermediate was recently reported in the hydrolysis of meropenem by di-Zn(II) SPM-1 [116]. Regarding mono-metallic variants, this intermediate has been show to accumulate in mono-Co(II) BcII with the metal at the Zn2 site [23]. Instead, a study on a

BcII variant showed that depletion of the Zn2 site resulted in a loss of the enzyme activity due to the inability to stabilize this intermediate, definitively proving the essentiality of the Zn2 site in catalysis [24].

2.2 Mechanism of B2 Metallo-β-lactamases

B2 MBLs are efficient carbapenemases, with poor activity against penicillins and cephalosporins [117–119]. These enzymes (CphA, ImiS and Sfh-I) show their maximum activity in the mono-Zn(II) form, while binding of a second Zn(II) ion inhibits them to different degrees depending on their metal binding affinities (see below). The crystal structures of CphA and Sfh-I revealed that the tightly bound Zn(II) ion is located on the M2 site [61,62]. Another distinctive feature of these structures is the presence of an α-helix on the edge of the active site groove and a group of hydrophobic residues that, together with this helix, define a hydrophobic wall on the active site [61,62], in contrast with the flexible loops present in B1 and B3 enzymes.

2.2.1 Mechanistic studies on B2 enzymes—Extensive mechanistic studies are available for the hydrolysis of imipenem and meropenem catalyzed by ImiS [120]. The activity of ImiS is not affected by pH in the 5.0–8.5 pH range, while proton inventories indicated at least one rate-limiting proton transfer, with a solvent kinetic effect of 1.7. Stopped-flow fluorescence studies on ImiS, which monitor changes in tryptophan fluorescence on the enzyme upon substrate binding, displayed biphasic time courses upon reaction with imipenem and meropenem, with the second, slower phase corresponding to substrate hydrolysis and product release, which could not be distinguished. Mechanistic studies on Co(II)-substituted ImiS showed no changes in the absorption spectrum of the metal site during turnover, despite RFQ-EPR studies supported accumulation of a reaction intermediate with a five-coordinate metal center. Unpublished pre-steady-state experiments from our group on the hydrolysis of imipenem by Zn(II)-Sfh-I disclosed the existence of transiently populated intermediates during the catalytic cycle, similar to the one reported for the reaction catalyzed by di-Zn(II) BcII (Figure 2B). Despite there might be differences between the distinct B2 enzymes, it is clear that carbapenem hydrolysis takes place by a reaction intermediate involving changes in the geometry of the only metal site present in these enzymes, i.e., the Zn2 site.

The crystal structure of Sfh-I at 1.33 Å allowed elucidating the arrangement of water molecules in the active site [62]. In this structure, the coordination sphere of Zn2 is completed by a single water molecule, with a Zn2-Wat2 distance (2.24 Å; Table 1) consistent with a water molecule rather than with a hydroxide. The Zn1 site is occupied by a second water molecule (Wat1), involved in a hydrogen bond network, with a particularly strong interaction with His118 (O-Nδ1 2.0 Å) that suggests water activation by this His residue, despite involvement of Asp120 cannot be discarded [61].

The Zn(II) ion steers substrate binding to the carboxylate group, aided by a positively charged residue in position 224, conserved in B2 enzymes. Wat1 is thus expected to be the attacking nucleophile (Figure 3), resulting in the opening of the β-lactam ring to form an anionic intermediate [62], analogous to the mechanism proposed for dinuclear enzymes

(Figure 2B). Protonation of this intermediate can occur on N1 (in a buried, less accessible position) or on C3, giving rise to different tautomers. Impaired proton transfer in B2 MBLs implies that the anionic intermediate can accumulate during carbapenem hydrolysis, as is the case in the B1 and B3 enzymes. This is consistent with the spectroscopic features of the intermediate observed using stopped-flow coupled to a PDA detector in Sfh-I (unpublished results from our group). This intermediate can also be related to the one found on imipenem hydrolysis by ImiS using rapid-freeze quench EPR [120].

In summary, the main mechanistic difference of B2 enzymes with the dinuclear B1 and B3 MBLs is the fact that the metal ion is not involved in the activation of the water nucleophile. However, the two-fold role of Zn(II) in B2 enzymes in binding the substrate and stabilizing the anionic intermediate resembles the role proposed for the Zn2 site in B1 and B3 enzymes, despite the different active site topologies and metal site content.

2.2.2 The inhibitory site of B2 enzymes—The His116Asn change in B2 MBLs abolishes productive binding of Zn(II) at the M1 site, removing a conserved His ligand in B1 and B3 enzymes. All B2 enzymes bind a second Zn(II) equivalent, with dissociation constants ranging from a surprisingly low value of 15 nM in ImiS [118] to 40–90 μM in CphA [117] and Sfh-I [119]. The effect of the second Zn(II) equivalent in the carbapenem activity is also different, showing inhibition in CphA and ImiS, and no effect for Sfh-I.

The structure of di-Zn(II) CphA showed that the second inhibitory Zn(II) ion binds to a slightly modified M1 site, through coordination to His196 and His118 [47]. From this structure it was proposed that binding of the second Zn(II) ion to His118 and His196 would prevent them from playing a key role in the hydrolysis of carbapenems catalyzed by B2 MBLs. This coordination geometry is consistent with the inhibition at μM Zn(II) observed for CphA, but not for ImiS. The essentiality of these residues in catalysis is supported by the very weak activities of the H118A and H196A mutants [63]. Hence, B2 enzymes can bind a second Zn(II) ion at a modified M1 site, giving rise though to an inactive form since the metal at this site is not capable of fulfilling the role of Zn1 in B1 and B3 enzymes. The structure of di-Zn(II) CphA indeed suggests that Asn in position 116 precludes properly positioning of the Zn1 ion to activate the nucleophilic water molecule, and sequesters residues His 118 and His 196 impeding their participation in the catalytic mechanism as seen in the active mono-nuclear form of B2 enzymes.

3 Crystal structures with hydrolyzed substrates

3.1 Crystal structure of NDM-1 in complex with various hydrolyzed penicillins and hydrolyzed meropenem

The crystal structure of the B1 enzyme NDM-1 was solved in complex with several hydrolyzed penicillins: ampicillin [59], methicillin, benzylpenicillin, and oxacillin [44]. These structures feature some important similarities: all of them present a water/hydroxide molecule bridging both Zn(II) ions, with a longer Zn1-Zn2 distance than in the resting state, always with a weaker interaction with Zn2 (Table 2 and Figure 4D). The complexes with hydrolyzed penicillins present the longest distances (4.6 Å) reported for a dinuclear MBL (Table 1).

The R1 functional groups display variable conformations, while the orientation of the β-lactam core is identical in all the product complexes. The hydrolyzed antibiotics contain two carboxylate groups: the conserved C3-carboxylate, and the C7-carboxylate (this one is generated after hydrolysis of the amide bond). The C3-carboxylate coordinates Zn2 and forms a salt bridge with Lys224. The nitrogen atom of the β-lactam ring (N4) is positioned on top of Zn2 at a bonding distance of 2.2 Å (Table 2 and Figure 4D). The interaction of Zn2 with these two moieties is present in all enzyme-product complexes and is in agreement with the proposed substrate binding mode and reaction intermediates. One of the oxygen atoms of the C7 carboxylate is bound to Zn1, while the other oxygen is involved in a hydrogen bond interaction with Asn233, conserved among B1 and B2 enzymes [39]. The bulky R1 groups of methicillin and oxacillin are accommodated on the active site cleft, between the L3- and L10-loops, which is enlarged with respect to other B1 MBLs [44].

The complex of NDM with hydrolyzed meropenem, instead, reveals a somehow different scenario [44]. The direct coordination of the carbapenem C3 carboxylate and the N4 atom with the Zn2 ion are preserved (Table 2), while the major difference resides in the position of the newly formed C7 carboxylate. This moiety is found bridging the two Zn(II) ions (at 2.2 and 2.6 Å from Zn1 and Zn2, respectively), giving rise to a tetrahedral Zn1 site and a hexa-coordinate Zn2 site in the product complex. As a result, there is no water/hydroxide in this position and the Zn1-Zn2 distance is shorter than in the other complexes, but still larger than in the resting form (4.0 Å, see Table 2). Another structure deposited by Kim et al. (PDB 4RBS) of NDM-1 in complex with meropenem shows a very similar disposition (see Table 2).

A common feature of these structures is that Wat2, binding Zn2 in the resting form, is replaced in the enzyme-product adducts by the interactions with the carboxylate and the nitrogen atom, expanding the coordination sphere of Zn2 and reflecting the ability of this site to bind negatively charged moieties. The presence of a water/hydroxide bridging the two Zn(II) ions after the nucleophilic attack [44,59] reflects the uptake of a new solvent molecule or the rearrangement of Wat2 into this position, as suggested in the proposed mechanisms (Figure 1B and Figure 2). This observation validates the proposal that this water molecule is the proton donor. The lack of a solvent molecule in the meropenem complex could be attributed to a possible protonation on the carbon atom in the intermediate within the active site by an incoming water molecule from the bulk. However, the electron density maps preclude assessing the protonation state and hybridization of the carbon atom in these adducts.

3.2 NDM-1 crystal structure in complex with a hydrolyzed cephalosporin and a cephalosporoate intermediate

The crystal structures of NDM-1 in complex with a cefuroxime intermediate and hydrolyzed cephalexin were solved at 1.3 and 2.0 Å, respectively [79]. The two hydrolyzed cephalosporins in complex with NDM-1 show very similar arrangements. In both cases, the bridging water/hydroxide molecule is present between the two Zn(II) ions (Figure 4I). The newly formed carboxylate group at C8 interacts with Zn1 and with Asn233. The nitrogen atom of the opened β-lactam ring (N5) and the C4-carboxylate are bound to Zn2, with the

latter also interacting with Lys224. The major difference is the Zn1-Zn2 distance, which is shorter for the cefuroxime intermediate (3.8 Å) than for the complex with cephalexin product (4.5 Å). Overall, the active site interactions resemble more closely those found in the enzyme-product adducts of NDM-1 with hydrolyzed penicillins than those with meropenem.

The hydrolysis of cephalosporins with good R2 leaving groups, like cefalotin, ceftazidime and cefoxitin, proceeds through: (i) tautomerization of the double bond in the dihydrothiazine ring from position 3–4 to 4–5 and (ii) protonation and elimination of the R2 group with formation of a new double bond 3–3′ (Figure 4H). This was demonstrated to be the case for cefuroxime, which presents a carbamoyl R2 group [79]. Surprisingly, in the structure of NDM-1 in complex with cefuroxime there was density for the carbamoyl group, suggesting that an intermediate step was captured (Figure 4I). The planarity among C6, N5, C4 and C16 indicates a shifted double bond from position 3–4 to 4–5 (Figure 4H). Also, C3 shows sp^3 hybridization, suggesting a transition from sp^2 in the substrate to sp^3 in the trapped species, and a double bond rearrangement. Feng et al. modeled an intermediate containing a negatively charged C3 with perfect density fitting. This anionic intermediate resembles the one proposed for nitrocefin [66] and imipenem [23] hydrolysis. In the case of nitrocefin, though the intermediate has been described as negatively charged on N5 atom [66], it is stabilized by delocalization through an extended π–conjugated system that includes the C3 and C4 atoms and the dinitrostyryl group of the R2 substituent [121]. In the case of the model proposed for imipenem, it would be equivalent to EI^2, in which the negative charge is localized at C3. At the same time, this intermediate strongly supports the proposal that the C-N bond cleavage and nitrogen protonation proceed in two separate steps, and that this last step is the rate-limiting one.

In the case of the cephalexin complex, the ligand electron density accommodates a hydrolyzed molecule displaying a C3 with sp^3 hybridization, suggesting full protonation of C3. Cephalexin lacks a good leaving group and therefore hydrolysis proceeds through a proton uptake at position 3.

3.3 L1 with hydrolyzed moxalactam

The crystal structure of L1 with the hydrolyzed form of the oxacephem antibiotic moxalactam was the first one of a di-Zn(II) MBL in complex with a hydrolyzed substrate [60]. Hydrolyzed moxalactam binds the enzyme through interactions with both Zn(II) ions and with side chains of residues adjacent to the active site (Figure 4E). Zn2 binds the β-lactam amide nitrogen and the C4 carboxylate, replicating the already reported features, while Zn1 interacts with the carboxylate group generated after hydrolysis of the β-lactam. The C4 carboxylate also interacts with Ser221 and Ser223, functionally equivalent to the Lys224 residue present in B1 and B2 MBLs [44,75,122], despite not being essential for catalysis [110].

The C8 carboxylate generated after β-lactam hydrolysis is a Zn1 ligand, which becomes penta-coordinate with a distorted trigonal bipyramidal geometry. The carboxylate at position C4 of the moxalactam displaces the “apical” water molecule (Wat2) present in the Zn2 coordination sphere in the resting enzyme while the β-lactam nitrogen atom (N5) approaches

from a direction opposite to His121. This arrangement supports a role for Zn2 in stabilizing the transient development of a negative charge on the N5 nitrogen atom. In addition, the structure shows a water/hydroxide molecule bridging the two metal ions, in line with the complexes of NDM-1 with hydrolyzed penicillins and cephalosporins.

3.4 CphA crystal structure in complex with hydrolyzed biapenem

Soaking of CphA crystals with biapenem allowed trapping of a bound species in the active site, resulting from a molecular rearrangement in the substrate after the nucleophilic attack [61]. As observed in the previously discussed adducts, the C-N β-lactam bond has already been cleaved, the N4 atom and the C3 carboxylate bind the Zn(II) ion, and the latter also interacts with Lys224 and with the backbone nitrogen atom of Asn233 (Table 2 and Figure 4F). The molecule has lost the double bond C2=C3 and has undergone an internal molecular rearrangement, with several hydrophobic contacts within the active site pocket.

A water molecule (Wat1) is located at 2.9 Å of the N4 of the intermediate and at 2.7 Å of His118, suggesting that the interaction with His118 can reduce the pKa of Wat1 sufficiently for it to act as the nucleophile or to transfer a proton to the intermediate (Figure 3). This interaction however is not as tight as the one reported for resting Sfh-I, that confirms this hypothesis (see Table 1 and Table 2). This structure is in line with the previously discussed mechanisms, and the observed rearrangement can be attributed to the unique nature of this substrate.

4 Concluding Remarks

The main difficulties to design inhibitors for MBLs have resided in the considerable structural differences among the active site of enzymes from the different subclasses, and the distinct requirements of Zn(II) ions for the activity. This review aims to cover in an integrated form, the different mechanistic and structural studies on MBLs from the three subclasses, B1, B2 and B3.

One of the most striking differences in the proposed mechanisms is the activation of the attacking nucleophile. Dinuclear B1 and B3 enzymes use Zn1 as a Lewis acid to generate a nucleophilic hydroxide in the active site, as reported for most Zn(II)-dependent hydrolases. In contrast, mono-Zn(II) B2 do not employ the metal ion for this purpose, but instead, rely on a hydrogen bond network in the active site. His118 and His196 are thus involved in nucleophile activation in all enzymes, either by coordinating Zn1 in dinuclear enzymes or by direct interaction with the nucleophile in mononuclear enzymes. The latter case applies as well to the native mono-Zn(II) B2 enzymes or to B1 and B3 in the mono- Zn2 form. MBLs use these essential residues in a modular form, in which the putative M1 site activates the nucleophile, in such a way that substrate binding and orientation is not expected to differ considerably among class B enzymes. As a consequence, the presence of a metal ion at the M1 site is not essential for hydrolysis in all MBLs, since the role of Zn1 in dinuclear enzymes (activation of the nucleophilic water molecule) can be fulfilled by a particular set and arrangement of residues in mononuclear B2 enzymes and in the mononuclear B3 enzyme GOB. It is still a matter of debate whether the mono-Zn1 MBLs are biologically relevant. In any case, the metal in the M1 site becomes essential for hydrolysis of β-lactams

in this mononuclear form of some B1 and B3 enzymes, being responsible for nucleophile activation and for the protonation step. The ligands of the now empty M2 site participate in a hydrogen-bond network to orient the nucleophile and to guide the second catalytic water molecule to the zinc ion after the substrate is bound. However, the finding that B1 enzymes are only active in the periplasm as di-Zn(II) enzymes questions whether in vitro studies on mono-Zn(II) enzymes could be translated to the in vivo active species.

The role and essentiality of Zn2 is preserved for all MBLs and against all types of β-lactam substrates (cf. Figures 1–3). Zn2 provides the main electrostatic anchoring for substrate binding, which can be aided by different positively charged or polar residues varying along the MBL family. Mechanistic, mutagenesis and crystallographic information also support the role of Zn2 in stabilizing a common anionic reaction intermediate, in which the C-N β-lactam bond has already been cleaved. The differences observed with the distinct substrates, penicillins, cephalosporins and carbapenems are due to their particular structure that impact differentially in the accumulation of this anionic species. In any case, these evidences point to common mechanistic features in all MBLs, regardless the disparate structures of the distinct β-lactam substrates and active sites.

Acknowledgments

MRM was recipient of a doctoral fellowship from CONICET. AJV and LIL are Staff members from CONICET. This work was supported by grants from ANPCyT to AJV and LIL, and the US National Institutes of Health (1R01AI100560) to AJV.

References

1. Fisher JF, Meroueh SO, Mobashery S. Bacterial resistance to beta-lactam antibiotics: compelling opportunism, compelling opportunity. Chem Rev. 2005; 105:395–424. [PubMed: 15700950]
2. Medeiros AA. Evolution and dissemination of beta-lactamases accelerated by generations of beta-lactam antibiotics. Clin Infect Dis. 1997; 24(Suppl 1):S19–45. [PubMed: 8994778]
3. Demain AL, Elander RP. The beta-lactam antibiotics: past, present, and future. Antonie Van Leeuwenhoek. 1999; 75:5–19. [PubMed: 10422578]
4. Walsh C. Molecular mechanisms that confer antibacterial drug resistance. Nature. 2000; 406:775–781. [PubMed: 10963607]
5. Page MG. Cephalosporins in clinical development. Expert Opinion on Investigational Drugs. 2004; 13:973–985. [PubMed: 15268635]
6. Singh GS. Beta-lactams in the new millennium. Part-I: monobactams and carbapenems. Mini Rev Med Chem. 2004; 4:69–92. [PubMed: 14754445]
7. Paterson DL, Bonomo RA. Extended-spectrum beta-lactamases: a clinical update. Clin Microbiol Rev. 2005; 18:657–686. [PubMed: 16223952]
8. Nordmann P, Naas T, Poirel L. Global Spread of Carbapenemase-producing *Enterobacteriaceae*. Emerging Infectious Diseases. 2011; 17:1791–1798. [PubMed: 22000347]
9. Boucher HW, Talbot GH, Benjamin DK Jr, Bradley J, Guidos RJ, Jones RN, Murray BE, Bonomo RA, Gilbert D. Infectious Diseases Society of America. 10 × ’20 Progress--development of new drugs active against gram-negative bacilli: an update from the Infectious Diseases Society of America. Clin Infect Dis. 2013; 56:1685–1694. [PubMed: 23599308]
10. Cain C. Rediscovering antibiotics. SciBX: Science-Business eXchange. 2012:5.
11. Hede K. Antibiotic resistance: An infectious arms race. Nature. 2014; 509:S2–S3. [PubMed: 24784426]
12. Walsh TR, Toleman MA, Poirel L, Nordmann P. Metallo-beta-lactamases: the quiet before the storm? Clin Microbiol Rev. 2005; 18:306–325. [PubMed: 15831827]

13. Crowder MW, Spencer J, Vila AJ. Metallo-beta-lactamases: novel weaponry for antibiotic resistance in bacteria. Acc Chem Res. 2006; 39:721–728. [PubMed: 17042472]
14. Drawz SM, Bonomo RA. Three Decades of β-Lactamase Inhibitors. Clin Microbiol Rev. 2010; 23:160–201. [PubMed: 20065329]
15. Sabath LD, Abraham EP. Zinc as a cofactor for cephalosporinase from Bacillus cereus 569. Biochem J. 1966; 98:11C–13C.
16. Bicknell R, Schäffer A, Waley SG, Auld DS. Changes in the coordination geometry of the active-site metal during catalysis of benzylpenicillin hydrolysis by Bacillus cereus beta-lactamase II. Biochemistry. 1986; 25:7208–7215. [PubMed: 3099831]
17. Bounaga S, Laws AP, Galleni M, Page MI. The mechanism of catalysis and the inhibition of the Bacillus cereus zinc-dependent beta-lactamase. Biochem J. 1998; 331:703–711. [PubMed: 9560295]
18. Fabiane SM, Sohi MK, Wan T, Payne DJ, Bateson JH, Mitchell T, Sutton BJ. Crystal structure of the zinc-dependent beta-lactamase from Bacillus cereus at 1.9 A resolution: binuclear active site with features of a mononuclear enzyme. Biochemistry. 1998; 37:12404–12411. [PubMed: 9730812]
19. de Seny D, Prosperi-Meys C, Bebrone C, Rossolini GM, Page MI, Noel P, Frère J-M, Galleni M. Mutational analysis of the two zinc-binding sites of the Bacillus cereus 569/H/9 metallo-beta-lactamase. Biochem J. 2002; 363:687–696. [PubMed: 11964169]
20. Rasia RM, Vila AJ. Structural determinants of substrate binding to Bacillus cereus metallo-beta-lactamase. J Biol Chem. 2004; 279:26046–26051. [PubMed: 15140877]
21. Badarau A, Page MI. The variation of catalytic efficiency of Bacillus cereus metallo-beta-lactamase with different active site metal ions. Biochemistry. 2006; 45:10654–10666. [PubMed: 16939217]
22. Llarrull LI, Tioni MF, Vila AJ. Metal content and localization during turnover in B. cereus metallo-beta-lactamase. J Am Chem Soc. 2008; 130:15842–15851. [PubMed: 18980306]
23. Tioni MF, Llarrull LI, Poeylaut-Palena AA, Martí MA, Saggu M, Periyannan GR, Mata EG, Bennett B, Murgida DH, Vila AJ. Trapping and characterization of a reaction intermediate in carbapenem hydrolysis by B. cereus metallo-beta-lactamase. J Am Chem Soc. 2008; 130:15852–15863. [PubMed: 18980308]
24. González JM, Meini M-R, Tomatis PE, Medrano Martín FJ, Cricco JA, Vila AJ. Metallo-β-lactamases withstand low Zn(II) conditions by tuning metal-ligand interactions. Nat Chem Biol. 2012; 8:698–700. [PubMed: 22729148]
25. Cuchural GJ, Malamy MH, Tally FP. Beta-lactamase-mediated imipenem resistance in Bacteroides fragilis. Antimicrob Agents Chemother. 1986; 30:645–648. [PubMed: 3492173]
26. Walsh TR, Hall L, Assinder SJ, Nichols WW, Cartwright SJ, MacGowan AP, Bennett PM. Sequence analysis of the L1 metallo-beta-lactamase from Xanthomonas maltophilia. Biochim Biophys Acta. 1994; 1218:199–201. [PubMed: 8018721]
27. Shannon K, King A, Phillips I. Beta-lactamases with high activity against imipenem and Sch 34343 from Aeromonas hydrophila. J Antimicrob Chemother. 1986; 17:45–50. [PubMed: 3485091]
28. Walsh TR, Neville WA, Haran MH, Tolson D, Payne DJ, Bateson JH, MacGowan AP, Bennett PM. Nucleotide and amino acid sequences of the metallo-beta-lactamase, ImiS, from Aeromonas veronii bv. sobria. Antimicrob Agents Chemother. 1998; 42:436–439. [PubMed: 9527802]
29. Rossolini GM, Franceschini N, Riccio ML, Mercuri PS, Perilli M, Galleni M, Frere JM, Amicosante G. Characterization and sequence of the Chryseobacterium (Flavobacterium) meningosepticum carbapenemase: a new molecular class B beta-lactamase showing a broad substrate profile. Biochem J. 1998; 332:145–152. [PubMed: 9576862]
30. Bellais S, Aubert D, Naas T, Nordmann P. Molecular and biochemical heterogeneity of class B carbapenem-hydrolyzing beta-lactamases in Chryseobacterium meningosepticum. Antimicrob Agents Chemother. 2000; 44:1878–1886. [PubMed: 10858348]
31. Morán-Barrio J, González JM, Lisa MN, Costello AL, Peraro MD, Carloni P, Bennett B, Tierney DL, Limansky AS, Viale AM, Vila AJ. The metallo-beta-lactamase GOB is a mono-Zn(II) enzyme with a novel active site. J Biol Chem. 2007; 282:18286–18293. [PubMed: 17403673]

32. Chen Y, Succi J, Tenover FC, Koehler TM. Beta-lactamase genes of the penicillinsusceptible Bacillus anthracis Sterne strain. J Bacteriol. 2003; 185:823–830. [PubMed: 12533457]
33. Bush K, Fisher JF. Epidemiological expansion, structural studies, and clinical challenges of new β-lactamases from gram-negative bacteria. Annu Rev Microbiol. 2011; 65:455–478. [PubMed: 21740228]
34. Johnson AP, Woodford N. Global spread of antibiotic resistance: the example of New Delhi metallo- -lactamase (NDM)-mediated carbapenem resistance. Journal of Medical Microbiology. 2013; 62:499–513. [PubMed: 23329317]
35. Rossolini GM, Condemi MA, Pantanella F, Docquier J-D, Amicosante G, Thaller MC. Metallo-β-Lactamase Producers in Environmental Microbiota: New Molecular Class B Enzyme in Janthinobacterium lividum. Antimicrob Agents Chemother. 2001; 45:837–844. [PubMed: 11181369]
36. Saavedra MJ, Peixe L, Sousa JC, Henriques I, Alves A, Correia A. Sfh-I, a Subclass B2 Metallo-β-Lactamase from a Serratia fonticola Environmental Isolate. Antimicrob Agents Chemother. 2003; 47:2330–2333. [PubMed: 12821491]
37. Stoczko M, Frère J-M, Rossolini GM, Docquier J-D. Postgenomic scan of metallo-beta-lactamase homologues in rhizobacteria: identification and characterization of BJP-1, a subclass B3 ortholog from Bradyrhizobium japonicum. Antimicrob Agents Chemother. 2006; 50:1973–1981. [PubMed: 16723554]
38. Walsh TR, Weeks J, Livermore DM, Toleman MA. Dissemination of NDM-1 positive bacteria in the New Delhi environment and its implications for human health: an environmental point prevalence study. Lancet Infect Dis. 2011; 11:355–362. [PubMed: 21478057]
39. Garau G, García-Sáez I, Bebrone C, Anne C, Mercuri P, Galleni M, Frère J-M, Dideberg O. Update of the Standard Numbering Scheme for Class B β-Lactamases. Antimicrob Agents Chemother. 2004; 48:2347–2349. [PubMed: 15215079]
40. Bebrone C. Metallo-beta-lactamases (classification, activity, genetic organization, structure, zinc coordination) and their superfamily. Biochem Pharmacol. 2007; 74:1686–1701. [PubMed: 17597585]
41. de Seny D, Heinz U, Wommer S, Kiefer M, Meyer-Klaucke W, Galleni M, Frere JM, Bauer R, Adolph HW. Metal ion binding and coordination geometry for wild type and mutants of metallo-beta -lactamase from Bacillus cereus 569/H/9 (BcII): a combined thermodynamic, kinetic, and spectroscopic approach. J Biol Chem. 2001; 276:45065–45078. [PubMed: 11551939]
42. Concha NO, Janson CA, Rowling P, Pearson S, Cheever CA, Clarke BP, Lewis C, Galleni M, Frère JM, Payne DJ, Bateson JH, Abdel-Meguid SS. Crystal structure of the IMP-1 metallo beta-lactamase from Pseudomonas aeruginosa and its complex with a mercaptocarboxylate inhibitor: binding determinants of a potent, broad-spectrum inhibitor. Biochemistry. 2000; 39:4288–4298. [PubMed: 10757977]
43. Garcia-Saez I, Docquier J-D, Rossolini GM, Dideberg O. The three-dimensional structure of VIM-2, a Zn-beta-lactamase from Pseudomonas aeruginosa in its reduced and oxidised form. J Mol Biol. 2008; 375:604–611. [PubMed: 18061205]
44. King DT, Worrall LJ, Gruninger R, Strynadka NCJ. New Delhi metallo-β-lactamase: structural insights into β-lactam recognition and inhibition. J Am Chem Soc. 2012; 134:11362–11365. [PubMed: 22713171]
45. Docquier J-D, Benvenuti M, Calderone V, Stoczko M, Menciassi N, Rossolini GM, Mangani S. High-resolution crystal structure of the subclass B3 metallo-beta-lactamase BJP-1: rational basis for substrate specificity and interaction with sulfonamides. Antimicrob Agents Chemother. 2010; 54:4343–4351. [PubMed: 20696874]
46. Hall BG, Salipante SJ, Barlow M. The metallo-beta-lactamases fall into two distinct phylogenetic groups. J Mol Evol. 2003; 57:249–254. [PubMed: 14629034]
47. Bebrone C, Delbrück H, Kupper MB, Schlömer P, Willmann C, Frère J-M, Fischer R, Galleni M, Hoffmann KMV. The Structure of the Dizinc Subclass B2 Metallo-β-Lactamase CphA Reveals that the Second Inhibitory Zinc Ion Binds in the Histidine Site. Antimicrob Agents Chemother. 2009; 53:4464–4471. [PubMed: 19651913]

48. Yong D, Toleman MA, Giske CG, Cho HS, Sundman K, Lee K, Walsh TR. Characterization of a new metallo-beta-lactamase gene, bla(NDM-1), and a novel erythromycin esterase gene carried on a unique genetic structure in Klebsiella pneumoniae sequence type 14 from India. Antimicrob Agents Chemother. 2009; 53:5046–5054. [PubMed: 19770275]
49. Lauretti L, Riccio ML, Mazzariol A, Cornaglia G, Amicosante G, Fontana R, Rossolini GM. Cloning and characterization of blaVIM, a new integron-borne metallo-beta-lactamase gene from a Pseudomonas aeruginosa clinical isolate. Antimicrob Agents Chemother. 1999; 43:1584–1590. [PubMed: 10390207]
50. Zhao W-H, Hu Z-Q. IMP-type metallo-β-lactamases in Gram-negative bacilli: distribution, phylogeny, and association with integrons. Crit Rev Microbiol. 2011; 37:214–226. [PubMed: 21707466]
51. Toleman MA, Simm AM, Murphy TA, Gales AC, Biedenbach DJ, Jones RN, Walsh TR. Molecular characterization of SPM-1, a novel metallo-β-lactamase isolated in Latin America: report from the SENTRY antimicrobial surveillance programme. J Antimicrob Chemother. 2002; 50:673–679. [PubMed: 12407123]
52. Lim HM, Pène JJ, Shaw RW. Cloning, nucleotide sequence, and expression of the Bacillus cereus 5/B/6 beta-lactamase II structural gene. J Bacteriol. 1988; 170:2873–2878. [PubMed: 3131315]
53. Rasmussen BA, Gluzman Y, Tally FP. Cloning and sequencing of the class B beta-lactamase gene (ccrA) from Bacteroides fragilis TAL3636. Antimicrob Agents Chemother. 1990; 34:1590–1592. [PubMed: 2121094]
54. Massidda O, Rossolini GM, Satta G. The Aeromonas hydrophila cphA gene: molecular heterogeneity among class B metallo-beta-lactamases. J Bacteriol. 1991; 173:4611–4617. [PubMed: 1856163]
55. Boschi L, Mercuri PS, Riccio ML, Amicosante G, Galleni M, Frère JM, Rossolini GM. The Legionella (Fluoribacter) gormanii metallo-beta-lactamase: a new member of the highly divergent lineage of molecular-subclass B3 beta-lactamases. Antimicrob Agents Chemother. 2000; 44:1538–1543. [PubMed: 10817705]
56. Yong D, Toleman MA, Bell J, Ritchie B, Pratt R, Ryley H, Walsh TR. Genetic and Biochemical Characterization of an Acquired Subgroup B3 Metallo-β-Lactamase Gene, blaAIM-1, and Its Unique Genetic Context in Pseudomonas aeruginosa from Australia. Antimicrob Agents Chemother. 2012; 56:6154–6159. [PubMed: 22985886]
57. Concha NO, Rasmussen BA, Bush K, Herzberg O. Crystal structure of the wide-spectrum binuclear zinc beta-lactamase from Bacteroides fragilis. Structure. 1996; 4:823–836. [PubMed: 8805566]
58. Nauton L, Kahn R, Garau G, Hernandez JF, Dideberg O. Structural insights into the design of inhibitors for the L1 metallo-beta-lactamase from Stenotrophomonas maltophilia. J Mol Biol. 2008; 375:257–269. [PubMed: 17999929]
59. Zhang H, Hao Q. Crystal structure of NDM-1 reveals a common β-lactam hydrolysis mechanism. FASEB J. 2011; 25:2574–2582. [PubMed: 21507902]
60. Spencer J, Read J, Sessions RB, Howell S, Blackburn GM, Gamblin SJ. Antibiotic recognition by binuclear metallo-beta-lactamases revealed by X-ray crystallography. J Am Chem Soc. 2005; 127:14439–14444. [PubMed: 16218639]
61. Garau G, Bebrone C, Anne C, Galleni M, Frère J-M, Dideberg O. A metallo-beta-lactamase enzyme in action: crystal structures of the monozinc carbapenemase CphA and its complex with biapenem. J Mol Biol. 2005; 345:785–795. [PubMed: 15588826]
62. Fonseca F, Bromley EHC, Saavedra MJ, Correia A, Spencer J. Crystal structure of Serratia fonticola Sfh-I: activation of the nucleophile in mono-zinc metallo-β-lactamases. J Mol Biol. 2011; 411:951–959. [PubMed: 21762699]
63. Bebrone C, Anne C, Kerff F, Garau G, De Vriendt K, Lantin R, Devreese B, Van Beeumen J, Dideberg O, Frère J-M, Galleni M. Mutational analysis of the zinc- and substrate-binding sites in the CphA metallo-beta-lactamase from Aeromonas hydrophila. Biochem J. 2008; 414:151–159. [PubMed: 18498253]

64. Dudev T, Lin, Dudev M, Lim C. First–Second Shell Interacgons in Metal Binding Sites in Proteins:_ A PDB Survey and DFT/CDM Calculations. J Am Chem Soc. 2003; 125:3168–3180. [PubMed: 12617685]

65. Estiu G, Suárez D, Merz KM. Quantum mechanical and molecular dynamics simulations of ureases and Zn beta-lactamases. J Comput Chem. 2006; 27:1240–1262. [PubMed: 16773613]

66. Wang Z, Fast W, Benkovic SJ. On the mechanism of the metallo-beta-lactamase from Bacteroides fragilis. Biochemistry. 1999; 38:10013–10023. [PubMed: 10433708]

67. Lindskog S, Coleman JE. The catalytic mechanism of carbonic anhydrase. Proc Natl Acad Sci USA. 1973; 70:2505–2508. [PubMed: 4200327]

68. Chen G, Edwards T, D'souza VM, Holz RC. Mechanistic studies on the aminopeptidase from Aeromonas proteolytica: a two-metal ion mechanism for peptide hydrolysis. Biochemistry. 1997; 36:4278–4286. [PubMed: 9100023]

69. Mock WL, Tsay JT. pK values for active site residues of carboxypeptidase A. Journal of Biological Chemistry. 1988; 263:8635. [PubMed: 3379037]

70. Bigley AN, Raushel FM. Catalytic Mechanisms for Phosphotriesterases. Biochim Biophys Acta. 2013; 1834:443–453. [PubMed: 22561533]

71. Liao R-Z, Yu J-G, Himo F. Reaction mechanism of the trinuclear zinc enzyme phospholipase C: a density functional theory study. J Phys Chem B. 2010; 114:2533–2540. [PubMed: 20121060]

72. Allen FH. The Cambridge Structural Database: a quarter of a million crystal structures and rising. Acta Crystallographica Section B Structural Science. 2002; 58:380–388. [PubMed: 12037359]

73. Badarau A, Page MI. Enzyme deactivation due to metal-ion dissociation during turnover of the cobalt-beta-lactamase catalyzed hydrolysis of beta-lactams. Biochemistry. 2006; 45:11012–11020. [PubMed: 16953588]

74. Badarau A, Page MI. Loss of enzyme activity during turnover of the Bacillus cereus beta-lactamase catalysed hydrolysis of beta-lactams due to loss of zinc ion. J Biol Inorg Chem. 2008; 13:919–928. [PubMed: 18449576]

75. Yanchak MP, Taylor RA, Crowder MW. Mutational analysis of metallo-beta-lactamase CcrA from Bacteroides fragilis. Biochemistry. 2000; 39:11330–11339. [PubMed: 10985778]

76. Garrity JD, Carenbauer AL, Herron LR, Crowder MW. Metal Binding Asp-120 in Metallo- β-lactamase L1 from Stenotrophomonas maltophilia Plays a Crucial Role in Catalysis. J Biol Chem. 2004; 279:920–927. [PubMed: 14573595]

77. Yamaguchi Y, Kuroki T, Yasuzawa H, Higashi T, Jin W, Kawanami A, Yamagata Y, Arakawa Y, Goto M, Kurosaki H. Probing the role of Asp-120(81) of metallo-beta-lactamase (IMP-1) by site-directed mutagenesis, kinetic studies, and X-ray crystallography. J Biol Chem. 2005; 280:20824–20832. [PubMed: 15788415]

78. Llarrull LI, Fabiane SM, Kowalski JM, Bennett B, Sutton BJ, Vila AJ. Asp-120 locates Zn2 for optimal metallo-beta-lactamase activity. J Biol Chem. 2007; 282:18276–18285. [PubMed: 17426028]

79. Feng H, Ding J, Zhu D, Liu X, Xu X, Zhang Y, Zang S, Wang D-C, Liu W. Structural and Mechanistic Insights into NDM-1 Catalyzed Hydrolysis of Cephalosporins. J Am Chem Soc. 2014

80. Dal Peraro M, Vila AJ, Carloni P. Protonation state of Asp120 in the binuclear active site of the metallo-β-lactamase from Bacteroides fragilis. Inorganic chemistry. 2003; 42:4245–4247. [PubMed: 12844290]

81. Crisp J, Conners R, Garrity JD, Carenbauer AL, Crowder MW, Spencer J. Structural basis for the role of Asp-120 in metallo-beta-lactamases. Biochemistry. 2007; 46:10664–10674. [PubMed: 17715946]

82. Rasia RM, Vila AJ. Exploring the role and the binding affinity of a second zinc equivalent in B. cereus metallo-beta-lactamase. Biochemistry. 2002; 41:1853–1860. [PubMed: 11827530]

83. Davies AM, Rasia RM, Vila AJ, Sutton BJ, Fabiane SM. Effect of pH on the active site of an Arg121Cys mutant of the metallo-beta-lactamase from Bacillus cereus: implications for the enzyme mechanism. Biochemistry. 2005; 44:4841–4849. [PubMed: 15779910]

84. Llarrull LI, Tioni MF, Kowalski J, Bennett B, Vila AJ. Evidence for a dinuclear active site in the metallo-beta-lactamase BcII with substoichiometric Co(II). A new model for metal uptake. J Biol Chem. 2007; 282:30586–30595. [PubMed: 17715135]

85. Aitha M, Marts AR, Bergstrom A, Møller AJ, Moritz L, Turner L, Nix JC, Bonomo RA, Page RC, Tierney DL, Crowder MW. Biochemical, mechanistic, and spectroscopic characterization of metallo-β-lactamase VIM-2. Biochemistry. 2014; 53:7321–7331. [PubMed: 25356958]
86. Yang H, Aitha M, Marts AR, Hetrick A, Bennett B, Crowder MW, Tierney DL. Spectroscopic and mechanistic studies of heterodimetallic forms of metallo-β-lactamase NDM-1. J Am Chem Soc. 2014; 136:7273–7285. [PubMed: 24754678]
87. Bicknell R, Waley SG. Cryoenzymology of Bacillus cereus beta-lactamase II. Biochemistry. 1985; 24:6876–6887. [PubMed: 3935166]
88. Hawk MJ, Breece RM, Hajdin CE, Bender KM, Hu Z, Costello AL, Bennett B, Tierney DL, Crowder MW. Differential Binding of Co(II) and Zn(II) to Metallo-β-Lactamase Bla2 from Bacillus anthracis. J Am Chem Soc. 2009; 131:10753–10762. [PubMed: 19588962]
89. Hu Z, Periyannan G, Bennett B, Crowder MW. Role of the Zn1 and Zn2 sites in metallobeta-lactamase L1. J Am Chem Soc. 2008; 130:14207–14216. [PubMed: 18831550]
90. Dal Peraro M, Llarrull LI, Rothlisberger U, Vila AJ, Carloni P. Water-assisted reaction mechanism of monozinc beta-lactamases. J Am Chem Soc. 2004; 126:12661–12668. [PubMed: 15453800]
91. Wang Z, Fast W, Benkovic SJ. Direct Observation of an Enzyme-Bound Intermediate in the Catalytic Cycle of the Metallo-β-Lactamase from Bacteroides fragilis. J Am Chem Soc. 1998; 120:10788–10789.
92. Yang H, Aitha M, Hetrick AM, Richmond TK, Tierney DL, Crowder MW. Mechanistic and spectroscopic studies of metallo-β-lactamase NDM-1. Biochemistry. 2012; 51:3839–3847. [PubMed: 22482529]
93. McManus-Munoz S, Crowder MW. Kinetic mechanism of metallo-beta-lactamase L1 from Stenotrophomonas maltophilia. Biochemistry. 1999; 38:1547–1553. [PubMed: 9931021]
94. Garrity JD, Bennett B, Crowder MW. Direct evidence that the reaction intermediate of metallo-beta-lactamase L1 is metal bound. Biochemistry. 2005; 44:1078–1087. [PubMed: 15654764]
95. Breece RM, Hu Z, Bennett B, Crowder MW, Tierney DL. Motion of the Zinc Ions in Catalysis by a di-Zinc Metallo-β-Lactamase. J Am Chem Soc. 2009; 131:11642–11643. [PubMed: 19653676]
96. Park H, Brothers EN, Merz KM. Hybrid QM/MM and DFT investigations of the catalytic mechanism and inhibition of the dinuclear zinc metallo-beta-lactamase CcrA from Bacteroides fragilis. J Am Chem Soc. 2005; 127:4232–4241. [PubMed: 15783205]
97. Kaminskaia NV, Spingler B, Lippard SJ. Intermediate in beta-lactam hydrolysis catalyzed by a dinuclear zinc(II) complex: relevance to the mechanism of metallo-beta-lactamase. J Am Chem Soc. 2001; 123:6555–6563. [PubMed: 11439042]
98. Wang Z, Benkovic SJ. Purification, characterization, and kinetic studies of a soluble Bacteroides fragilis metallo-beta-lactamase that provides multiple antibiotic resistance. J Biol Chem. 1998; 273:22402–22408. [PubMed: 9712862]
99. Dal Peraro M, Vila AJ, Carloni P, Klein ML. Role of zinc content on the catalytic efficiency of B1 metallo beta-lactamases. J Am Chem Soc. 2007; 129:2808–2816. [PubMed: 17305336]
100. Cook, PF. Enzyme Mechanism from Isotope Effects. CRC Press; 1991.
101. Lisa M-N, Hemmingsen L, Vila AJ. Catalytic role of the metal ion in the metallo-beta-lactamase GOB. J Biol Chem. 2010; 285:4570–4577. [PubMed: 20007696]
102. Rasia RM, Vila AJ, et al. Mechanistic study of the hydrolysis of nitrocefin mediated by B. cereus metallo-β-lactamase. Arkivoc. 2003; 3:507–516.
103. Moali C, Anne C, Lamotte-Brasseur J, Groslambert S, Devreese B, Van Beeumen J, Galleni M, Frère J-M. Analysis of the Importance of the Metallo-β-Lactamase Active Site Loop in Substrate Binding and Catalysis. Chemistry & Biology. 2003; 10:319–329. [PubMed: 12725860]
104. Griffin DH, Richmond TK, Sanchez C, Moller AJ, Breece RM, Tierney DL, Bennett B, Crowder MW. Structural and kinetic studies on metallo-β-lactamase IMP-1. Biochemistry. 2011; 50:9125–9134. [PubMed: 21928807]
105. Tomatis PE, Fabiane SM, Simona F, Carloni P, Sutton BJ, Vila AJ. Adaptive protein evolution grants organismal fitness by improving catalysis and flexibility. Proc Natl Acad Sci USA. 2008; 105:20605–20610. [PubMed: 19098096]

106. Scrofani SD, Chung J, Huntley JJ, Benkovic SJ, Wright PE, Dyson HJ. NMR characterization of the metallo-beta-lactamase from Bacteroides fragilis and its interaction with a tight-binding inhibitor: role of an active-site loop. Biochemistry. 1999; 38:14507–14514. [PubMed: 10545172]

107. Huntley JJ, Scrofani SD, Osborne MJ, Wright PE, Dyson HJ. Dynamics of the metallo-beta-lactamase from Bacteroides fragilis in the presence and absence of a tight-binding inhibitor. Biochemistry. 2000; 39:13356–13364. [PubMed: 11063572]

108. Huntley JJA, Fast W, Benkovic SJ, Wright PE, Dyson HJ. Role of a solvent-exposed tryptophan in the recognition and binding of antibiotic substrates for a metallo-beta-lactamase. Protein Sci. 2003; 12:1368–1375. [PubMed: 12824483]

109. Karsisiotis AI, Damblon CF, Roberts GCK. Solution structures of the *Bacillus cereus* metallo-β-lactamase BcII and its complex with the broad spectrum inhibitor *R* - thiomandelic acid. Biochemical Journal. 2013; 456:397–407. [PubMed: 24059435]

110. Carenbauer AL, Garrity JD, Periyannan G, Yates RB, Crowder MW. Probing substrate binding to metallo-beta-lactamase L1 from Stenotrophomonas maltophilia by using site-directed mutagenesis. BMC Biochem. 2002; 3:4. [PubMed: 11876827]

111. Aitha M, Richmond TK, Hu Z, Hetrick A, Reese R, Gunther A, McCarrick R, Bennett B, Crowder MW. Dilution of dipolar interactions in a spin-labeled, multimeric metalloenzyme for DEER studies. J Inorg Biochem. 2014; 136:40–46. [PubMed: 24742748]

112. Aitha M, Moritz L, Sahu ID, Sanyurah O, Roche Z, McCarrick R, Lorigan GA, Bennett B, Crowder MW. Conformational dynamics of metallo-β-lactamase CcrA during catalysis investigated by using DEER spectroscopy. J Biol Inorg Chem. 2015; 20:585–594. [PubMed: 25827593]

113. Fisher J, Charnas RL, Bradley SM, Knowles JR. Inactivation of the RTEM beta-lactamase from Escherichia coli. Interaction of penam sulfones with enzyme. Biochemistry. 1981; 20:2726–2731. [PubMed: 7018564]

114. Zafaralla G, Mobashery S. Evidence for a new enzyme-catalyzed reaction other than. beta.-lactam hydrolysis in turnover of a penem by the TEM-1 .beta.-lactamase. J Am Chem Soc. 1993; 115:4962–4965.

115. Tripathi R, Nair NN. Mechanism of Meropenem Hydrolysis by New Delhi Metallo β-Lactamase. ACS Catal. 2015; 5:2577–2586.

116. Brem J, Struwe WB, Rydzik AM, Tarhonskaya H, Pfeffer I, Flashman E, van Berkel SS, Spencer J, Claridge TDW, McDonough MA, Benesch JLP, Schofield CJ. Studying the active-site loop movement of the São Paolo metallo-β-lactamase-1. Chem Sci. 2015; 6:956–963. [PubMed: 25717359]

117. Hernandez Valladares M, Felici A, Weber G, Adolph HW, Zeppezauer M, Rossolini GM, Amicosante G, Frère JM, Galleni M. Zn(II) dependence of the Aeromonas hydrophila AE036 metallo-beta-lactamase activity and stability. Biochemistry. 1997; 36:11534– 11541. [PubMed: 9298974]

118. Crawford PA, Sharma N, Chandrasekar S, Sigdel T, Walsh TR, Spencer J, Crowder MW. Over-expression, purification, and characterization of metallo-beta-lactamase ImiS from Aeromonas veronii bv. sobria. Protein Expr Purif. 2004; 36:272–279. [PubMed: 15249050]

119. Fonseca F, Arthur CJ, Bromley EHC, Samyn B, Moerman P, Saavedra MJ, Correia A, Spencer J. Biochemical characterization of Sfh-I, a subclass B2 metallo-beta-lactamase from Serratia fonticola UTAD54. Antimicrob Agents Chemother. 2011; 55:5392–5395. [PubMed: 21876065]

120. Sharma NP, Hajdin C, Chandrasekar S, Bennett B, Yang K-W, Crowder MW. Mechanistic studies on the mononuclear ZnII-containing metallo-beta-lactamase ImiS from Aeromonas sobria. Biochemistry. 2006; 45:10729–10738. [PubMed: 16939225]

121. Spencer J, Clarke AR, Walsh TR. Novel Mechanism of Hydrolysis of Therapeutic β-Lactams byStenotrophomonas maltophilia L1 Metallo-β-lactamase. J Biol Chem. 2001; 276:33638–33644. [PubMed: 11443136]

122. Haruta S, Yamamoto ET, Eriguchi Y, Sawai T. Characterization of the active-site residues asparagine 167 and lysine 161 of the IMP-1 metallo beta-lactamase. FEMS Microbiol Lett. 2001; 197:85–89. [PubMed: 11287151]

123. King D, Strynadka N. Crystal structure of New Delhi metallo-β-lactamase reveals molecular basis for antibiotic resistance. Protein Sci. 2011; 20:1484–1491. [PubMed: 21774017]

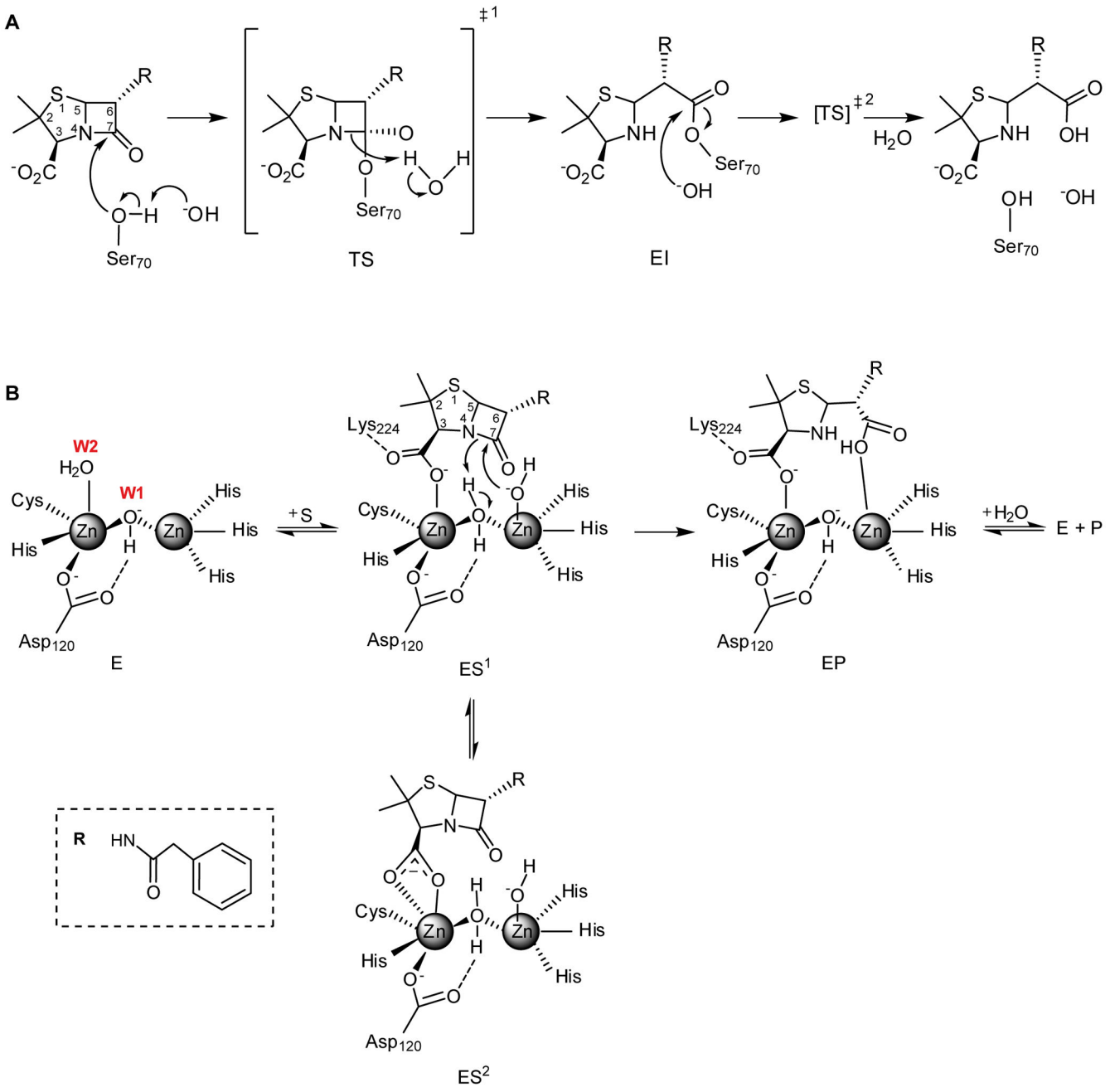

Figure 1.

A) Reaction mechanism for penicillin hydrolysis by class A serine-β-lactamases. This reaction scheme is based in the one reported in reference [14], which reviews original data.

B) Reaction mechanism for penicillin hydrolysis by di-Zn(II) B1 enzymes. The reaction scheme is based on the results on penicillin G hydrolysis by di-Co(II)-BcII from reference [22]. The representation of E is taken from the crystallographic structures of di-Zn(II) BcII (PDB 1BC2) and di- Co(II) BcII (PDB 3I11). The representation of EP is based on the crystallographic structures of NDM- 1 complexed with hydrolyzed penicillins (see section 3.1). W1 stands for Wat1 and W2 stands for Wat2.

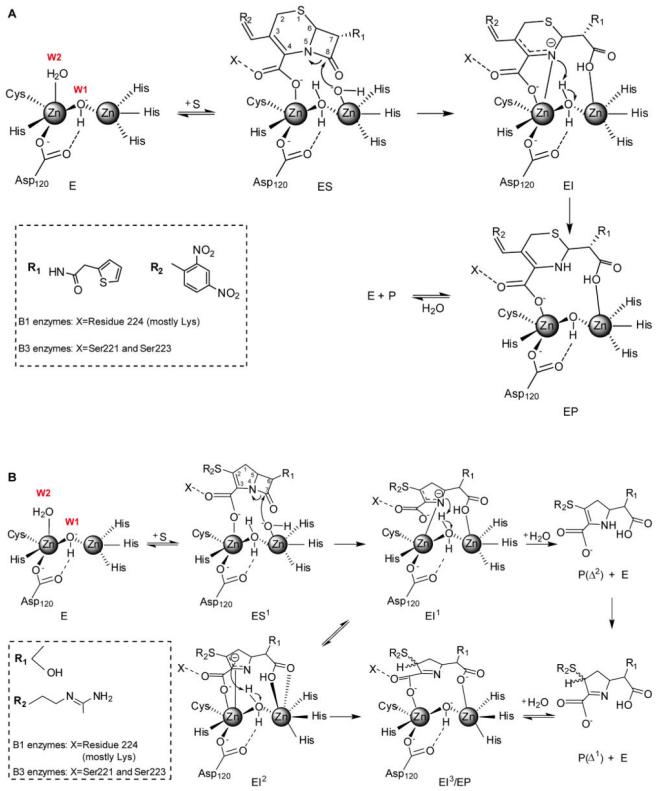

Figure 2.

A) Reaction mechanism for nitrocefin hydrolysis by di-Zn(II) B1 and B3 enzymes. EI is the experimentally characterized anionic intermediate interacting with Zn2 via the N atom and the carboxylate [66,91]. The same scheme would be valid for other chromogenic cephalosporins such as cromaceph and CENTA [92]. **B) Reaction mechanism for imipenem hydrolysis by di-Zn(II) B1 and B3 enzymes.** EI^1 and EI^2 are the experimentally characterized anionic intermediates [23], stabilized by interaction with Zn2. The representation of EI^2 is based on the crystallographic structures of NDM-1 in complex with hydrolyzed meropenem (PDB 4EYL, see Figure 4) [44]. W1 stands for Wat1 and W2 stands for Wat2.

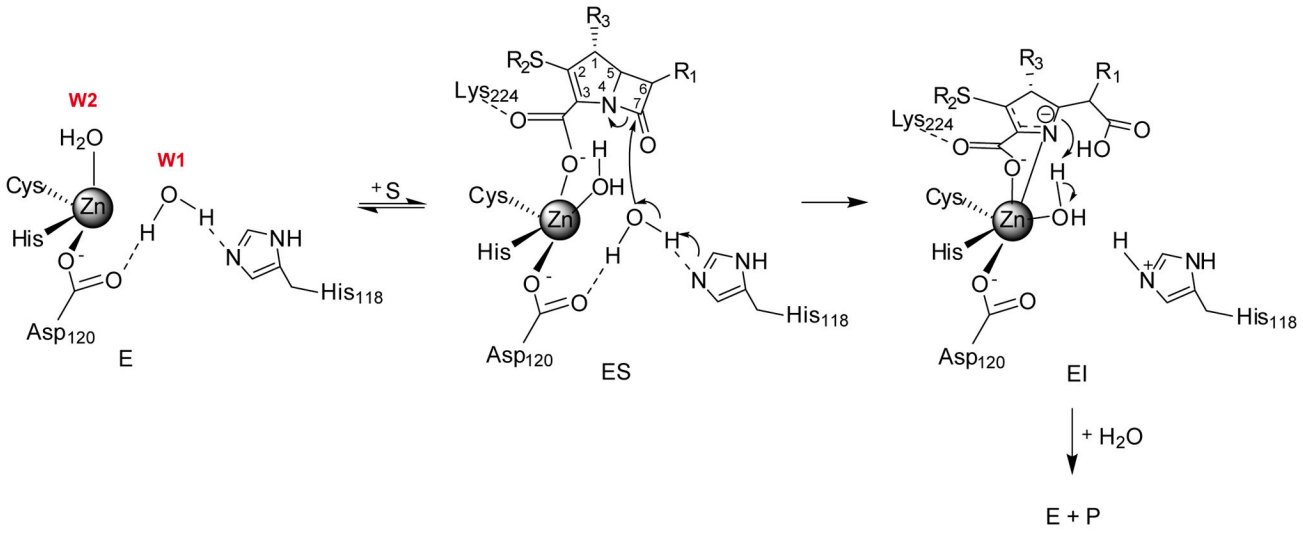

Figure 3. Minimum reaction mechanism for carbapenem hydrolysis by mono-Zn(II)-B2 enzymes

The arrangement of water molecules is based on the crystallographic structures of CphA, free and in complex with hydrolyzed biapenem [47,61], and of the free form of Sfh-I [62]. W1 stands for Wat1 and W2 stands for Wat2.

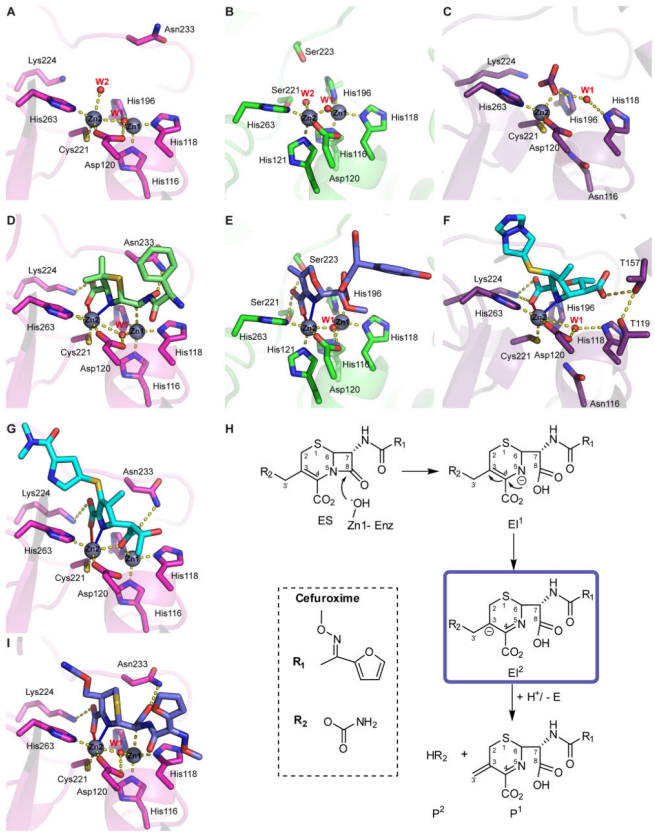

Figure 4. Active sites of free, EI and EP adducts solved by crystallography

A) Free form of NDM-1 (PDB 3SPU). **B)** Free form of L1 (PDB 2FM6). **C)** Free form of CphA (PDB 1X8G). **D)** NDM-1 in complex with hydrolyzed ampicillin (PDB 3Q6X) **E)** L1 in complex with hydrolyzed moxolactam (PDB 2AIO). **F)** CphA in complex with hydrolyzed biapenem (PDB 1X8I). **G)** NDM-1 in complex with hydrolyzed meropenem (4EYL). **H)** Reaction mechanism for hydrolysis of cephalosporins with good R2 leaving groups (*i.e.*, cefuroxime) by NDM-1 [79]. **I)** NDM-1 in complex with a cefuroxime hydrolysis intermediate (4RLO) corresponding to species EI^2 in panel H. W1 stands for Wat1 and W2 stands for Wat2.

Table 1

Relevant distances in the active sites of MBLs in their free forms from X-ray crystallography.

Free Forms				Distance (Å)				
PDB code	**Enzyme (subclass)**	**Resolution (Å)**	**Reference**	**Chain**	**Zn1-Zn2**	**Wat1-Zn1**	**Wat1-Zn2**	**Wat2-Zn2**
3SPU	NDM-1 (B1)	2.1	[123]	A	3.8	2.5	2.5	2.5
				B	3.9	1.9	2.6	2.7
2FM6	L1 (B3)	1.8	[58]	A	3.5	1.9	1.9	2.5
				B	3.5	1.8	2.1	2.5

					Wat1-H118	**Wat1-D120**	**Wat1-H196**	**Wat1-Zn2**	**Wat2-Zn2**
1X8G	CphA (B2)	1.7	[61]		3.1	3.4	4.4	4.0	-
3SD9	Sfh-I (B2)	1.9	[62]	A	2.0	3.8	2.5	3.5	2.2
				B	2.0	4.4	2.4	3.4	2.3

FEBS Lett. Author manuscript; available in PMC 2016 November 14.

Table 2

Relevant distances in the active sites of MBLs in EP[a] or EI[b] complexes from X-ray crystallography.

Penicillins					Distance (Å)								
PDB code	**Enzyme**	**Resolution (Å)**	**Hydrolized β-lactam**	**Reference**	**Chain**	**Zn1-Zn2**	**Wat1-Zn1**	**Wat1-Zn2**	**Wat2-Zn2**	**C7O-Zn1**	**C7O-Zn2**	**C3O-Zn2**	**N4-Zn2**
3Q6X	NDM-1[a] (B1)	1.3	ampicillin	[59]	A	4.6	2.1	3.0	-	2.4	4.3	2.2	2.2
					B	4.6	2.0	3.0	-	2.5	4.3	2.2	2.2
4EYF	NDM-1[a] (B1)	1.8	penicillin G	[44]	A	4.6	1.9	3.1	-	2.5	4.4	2.2	2.2
					B	4.6	2.0	3.1	-	2.4	4.4	2.1	2.2
4EY2	NDM-1[a] (B1)	1.2	methicillin	[44]	A	4.6	2.0	3.0	-	2.5	4.4	2.2	2.1
					B	4.6	2.0	3.0	-	2.5	4.4	2.2	2.2
4EYB	NDM-1[a] (B1)	1.2	oxacillin	[44]	A	4.5	2.0	2.9	-	2.5	4.4	2.2	2.1
					B	4.6	2.0	3.0	-	2.5	4.4	2.1	2.1

Cephalosporins													
PDB code	**Enzyme**	**Resolution (Å)**	**Hydrolized β-lactam**	**Reference**	**Chain**	**Zn1-Zn2**	**Wat1-Zn1**	**Wat1-Zn2**	**Wat2-Zn2**	**C8O-Zn1**	**C8O-Zn2**	**C4O-Zn2**	**N5-Zn2**
2AIO	L1 (B3)[a]	1.7	moxalactam	[60]		3.7	2.0	2.2	-	2.4	4.2	2.3	2.4
4RL0	NDM-1[b] (B1)	1.3	cefuroxime	[79]	A	3.8	2.0	2.2	-	2.8	4.2	2.1	2.4
					B	3.8	2.0	2.2	-	2.9	4.2	2.2	2.3
4RL2	NDM-1[a] (B1)	2.0	cephalexin	[79]	A	4.5	1.8	3.0	-	2.5	4.3	2.3	2.4
					B	4.5	2.0	2.8	-	2.4	4.3	2.3	2.4

Carbapenems													
PDB code	**Enzyme**	**Resolution (Å)**	**Hydrolized β-lactam**	**Reference**	**Chain**	**Zn1-Zn2**	**Wat1-Zn1**	**Wat1-Zn2**	**Wat2-Zn2**	**C7O-Zn1**	**C7O-Zn2**	**C3O-Zn2**	**N4-Zn2**
4EYL	NDM-1[a] (B1)	1.9	meropenem	[44]	A	4.0	-	-	-	2.3	2.5	3.0	2.2
					B	3.9	-	-	-	2.2	2.7	2.9	2.3
4RBS	NDM-1[a] (B1)	2.4	meropenem	To be published (Kim, Y. et al)	A	4.0	-	-	-	2.0	3.3	3.0	2.1
					B	4.0	-	-	-	2.2	3.0	3.1	2.1
							Wat1-H118	**Wat1-D120**	**Wat1-H196**	**Wat1-Zn2**	**Wat2-Zn2**	**C3O-Zn2**	**N4-Zn2**
1X8I	CphA (B2)[a]	1.9	biapenem	[61]			2.7	2.8	4.0	3.4	-	2.4	2.2